
INCLUSIVE TRAINING SEPARATION AND IMPLICIT KNOWLEDGE INTERACTION FOR BALANCED ONLINE CLASS-INCREMENTAL LEARNING

Shunjie Wen
Inha University
wenshunjie@inha.edu

Thomas Heinis
Imperial College London
t.heinis@imperial.ac.uk

Dong-Wan Choi
Inha University
dchoi@inha.ac.kr

April 30, 2025

ABSTRACT

Online class-incremental learning (OCIL) focuses on gradually learning new classes (called *plasticity*) from a stream of data in a single-pass, while concurrently preserving knowledge of previously learned classes (called *stability*). The primary challenge in OCIL lies in maintaining a good balance between the knowledge of old and new classes within the continually updated model. Most existing methods rely on *explicit* knowledge interaction through *experience replay*, and often employ *exclusive* training separation to address bias problems. Nevertheless, it still remains a big challenge to achieve a well-balanced learner, as these methods often exhibit either reduced plasticity or limited stability due to difficulties in continually integrating knowledge in the OCIL setting. In this paper, we propose a novel replay-based method, called **Balanced Online Incremental Learning (BOIL)**, which can achieve both high plasticity and stability, thus ensuring more balanced performance in OCIL. Our BOIL method proposes an *inclusive* training separation strategy using dual classifiers so that knowledge from both old and new classes can effectively be integrated into the model, while introducing *implicit* approaches for transferring knowledge across the two classifiers. Extensive experimental evaluations over three widely-used OCIL benchmark datasets demonstrate the superiority of BOIL, showing more balanced yet better performance compared to state-of-the-art replay-based OCIL methods.

1 Introduction

Online class-incremental learning (OCIL) has attracted considerable attention in the deep learning community, enabling knowledge accumulation of new classes over time. Unlike its offline counterpart, which assumes access to a complete training set for each task, OCIL is given a single-pass stream where the learner is allowed to view each mini-batch of the task only once. This partial accessibility of data makes OCIL more appealing in practice but also brings a greater challenge in addressing the core problem of continual learning: *stability-plasticity* dilemma [1], i.e., balancing knowledge preservation (stability) with knowledge acquisition (plasticity). Due to the limited training opportunities with on-the-fly samples in OCIL, the model can easily be biased toward new classes without a careful strategy of knowledge preservation. Conversely, a strong policy to preserve past information can severely impair the learning performance due to the small number of incoming samples.

The majority of OCIL methods tackle this challenge by using *experience replay* (ER) [2], which trains a mix batch of incoming samples from the stream and previous ones that are partially stored in a memory buffer. However, this *explicit* knowledge interaction via sample blending cannot completely resolve the stability-plasticity dilemma, since class imbalance is inevitable in OCIL with a fixed buffer size. As learning progresses over time, it would become more difficult to maintain balanced performance only by joint training with mix batches.

To alleviate this imbalance issue in OCIL, existing replay-based methods incorporate their additional techniques, generally falling into two categories. The first category is *training distinction* [3, 4, 5, 6, 7, 8, 9], which imposes different training policies or losses on buffer samples and new samples, respectively. Most works in this category focus on how to avoid the trained model being biased toward new classes by loss separation [3, 4, 9]. However, this

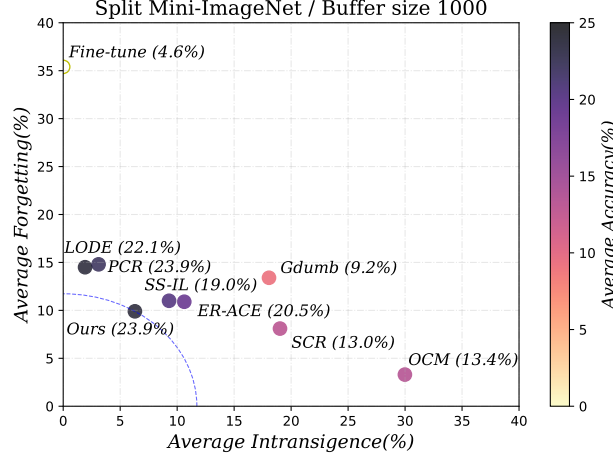


Figure 1: **Balance comparison in various OCIL methods on Split Mini-ImageNet ($\mathcal{M} = 1\text{K}$).** The color of the circle indicates the average accuracy. Lower forgetting and intransigence indicates better stability and higher plasticity, respectively. Our method (BOIL) is closest to the bottom-left corner with the highest accuracy, implying the most balanced and outperforming performance.

conversely tends to reduce the learning performance, as the conflicting tasks of learning new classes and replaying buffer samples are *competitively* and *exclusively* performed within a single classifier, without complementing each other. The second category is *feature enhancement* [10, 11, 12, 13, 14] that aims to obtain a more discriminative feature space where all embeddings, corresponding to either old classes or new classes, are well separated for better classification. This is typically done by using contrastive loss [11], as a replacement of cross-entropy loss, and by employing a post-hoc classifier, such as the nearest-class-mean (NCM) classifier [15], which takes the best use of well-separated features. However, in the OCIL setting with a limited number of samples, it is challenging to maintain historical feature information, as there are fewer pairs available for effective contrastive learning.

To overcome these limitations, this paper proposes a novel replay-based OCIL method, called **Balanced Online Incremental Learning (BOIL)**, designed to achieve a balanced yet satisfactory performance. Rather than competitively applying training policies or loss functions, our strategy is to incorporate separated components within the model itself, allowing for *inclusive separation* yet clearer differentiation across the tasks of knowledge acquisition and preservation. Specifically, we employ dual classifiers with identical structures: the *stream classifier*, which is dedicated to learning from new samples, and the *buffer classifier*, which focuses on preserving existing knowledge using buffered samples. This structural separation not only enables each classifier to concentrate on its corresponding task, but also facilitates learning knowledge across old and new classes, thereby enhancing knowledge acquisition and consolidation.

For transferring knowledge across tasks, we introduce *implicit* techniques that enable effective knowledge exchange between the dual classifiers, beyond simply blending old and new samples. Our first approach is redesigning *proxy-anchor loss* (PAL) [16], so that the weights of the stream classifier are treated as if they are learnable proxies during training with the shared feature extractor. This method supports forward transfer by leveraging the previous knowledge of the feature extractor to guide the training of the stream classifier. For backward transfer, we employ a momentum-based updating mechanism that gradually transfers adaptive information from the stream classifier to the buffer classifier. With these techniques, both classifiers implicitly exchange and integrate their acquired knowledge.

As summarized in Figure 1, our empirical study shows that the proposed BOIL method not only outperforms state-of-the-art OCIL methods in terms of overall performance (measured by average accuracy), but also clearly achieves the best balance between plasticity (measured by average intransigence) and stability (measured by average forgetting).

2 Related Works

Both online and offline continual learning (CL) typically focus on three major learning scenarios: class-incremental learning [17, 18, 19], task-incremental learning [18], and domain-incremental learning [20]. This paper specifically deals with online class-incremental learning (OCIL), which is practically appealing for real-world applications but more challenging due to the streaming nature of data.

Experience Replay. Similar to the widely-used rehearsal method [21, 10, 22, 18] in offline CL, *experience replay* (ER) [2] is considered the most effective approach in OCIL. The baseline ER method utilizes a bounded memory buffer to store and replay historical samples while jointly learning from new samples. As ER inevitably encounters imbalance issues between the streaming and buffered samples due to the bounded buffer, existing OCIL methods have introduced additional techniques, such as *training distinction* and *feature enhancement*.

Training Distinction. A number of existing works [6, 3, 23, 4, 9] can be classified as training distinction, which intends to apply different training policies or loss functions to buffer samples and stream samples to re-balance their contributions. For instance, [3] introduces loss separation, where losses for old and new classes are computed and backpropagated exclusively using a separated softmax function. Similarly, [4] proposes an asymmetric cross-entropy loss to avoid the drastic drift in old features caused by new incoming batches. While these approaches can help address imbalance issues mostly by prioritizing previous samples, their exclusive separation scheme within a single classifier can hinder the model’s ability to learn new knowledge as well as knowledge between old and new classes. Recently, [9] attempts to smooth this exclusive separation by carefully decoupling the cross-entropy loss for stream samples into two terms, one for only new classes and the other for old and new classes, while all the loss terms are still applied to a single classifier.

Feature Enhancement. Another group [11, 13, 12, 14] focuses on feature enhancement, aiming to construct a more discriminative feature space by correcting or discarding biased features learned through cross-entropy loss. [11] leverages supervised contrastive loss for representation learning and employs the NCM classifier at inference time. [12] explores the coupling of proxy-based and contrastive-based loss by replacing anchor samples with proxies in contrastive loss. [13] introduces mutual information maximization with InfoNCE loss to overcome catastrophic forgetting in online CL. Similarly, [14] utilizes InfoNCE but introduces online prototype learning to obtain representative features. However, compared to cross-entropy loss, contrastive learning typically requires extensive sample comparisons, which is challenging in OCIL with the bounded buffer.

3 Problem Statement

Problem Setting. In OCIL, we are given a sequence of tasks $\mathcal{D} = \{\mathcal{D}_t\}_{t=1}^T$ from a single-pass data stream. Each task t is associated with its dataset $\mathcal{D}_t = \{\mathcal{X}_t \times \mathcal{Y}_t\}$, where \mathcal{X}_t and \mathcal{Y}_t represent samples and corresponding labels, respectively. Without overlapping classes across tasks, each task t corresponds to a set C_t of classes such that $|C_t|$ is the same for all tasks. For the replay method, we also maintain a bounded memory buffer \mathcal{M} that stores some of the previously trained samples, which is therefore updated over the learning steps. At each learning step, the learner can access only a mini-batch $\mathcal{B}_\mathcal{D} \cup \mathcal{B}_\mathcal{M}$, where $\mathcal{B}_\mathcal{D}$ is a stream batch incoming from \mathcal{D} and $\mathcal{B}_\mathcal{M}$ is a buffer batch retrieved from \mathcal{M} . Throughout the entire process, every instance in \mathcal{D} can belong to only one stream batch $\mathcal{B}_\mathcal{D}$, and each $\mathcal{B}_\mathcal{D}$ can be trained only once.

Baseline OCIL. The general neural network architecture $\Theta = \{\Phi, \mathbf{W}\}$ for OCIL consists of a feature extractor h and a classifier f , parameterized by Φ and \mathbf{W} , respectively. For each input \mathbf{x} , we predict its label based on the corresponding logit vector $\mathbf{s} = f(\mathbf{z}; \mathbf{W})$, where $\mathbf{z} = h(\mathbf{x}; \Phi)$ is its feature embedding. Given a data stream \mathcal{D} containing T tasks and a target neural network Θ , the baseline replay-based OCIL aims to continuously train Θ with each \mathcal{D}_t for $t \in [1, T]$ such that Θ can make precise predictions for all the classes in T tasks, by optimizing the following objective function:

$$\arg \min_{\Phi, \mathbf{W}} \mathbb{E}_{(\mathbf{x}, y) \sim \mathcal{D}_t \cup \mathcal{M}} [\mathcal{L}_{CE}(y, f(h(\mathbf{x}; \Phi); \mathbf{W}))].$$

$\mathcal{L}_{CE}(y, \mathbf{s}) = -\log \frac{\exp(\mathbf{s}^{(y)})}{\sum_{j \in C_{1:t}} \exp(\mathbf{s}^{(j)})}$ is cross-entropy loss, where $C_{1:t} = \cup_{i=1}^t C_i$ indicates all the classes learned so far and $\mathbf{s}^{(j)}$ is the individual logit value of class j .

4 Methodology

In this section, we present our proposed BOIL method, which consists of two major components: (i) training separation with dual classifiers and (ii) implicit knowledge interaction. Intuitively, our techniques are motivated by both training distinction and feature enhancement, while introducing our novel approaches to address their limitations. The overall framework is illustrated in Figure 2.

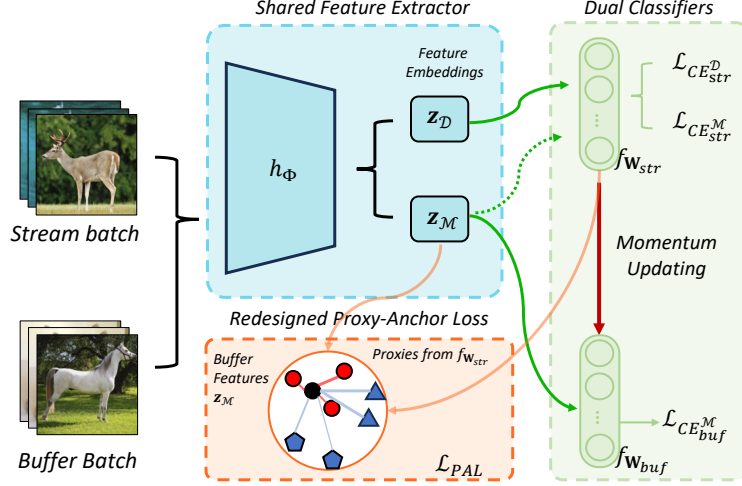


Figure 2: **Training overview of our BOIL method.** For each batch of stream and buffer samples, the shared feature extractor outputs corresponding features, which are then respectively fed into either stream or buffer classifier for separated training. Our redesigned proxy-anchor loss and momentum updating are used for implicit knowledge exchange, helping both forward and backward knowledge transfer and better discrimination ability. Green arrows represent the flow of features. Orange arrows indicate interactions between buffer features and the proxies from the stream classifier.

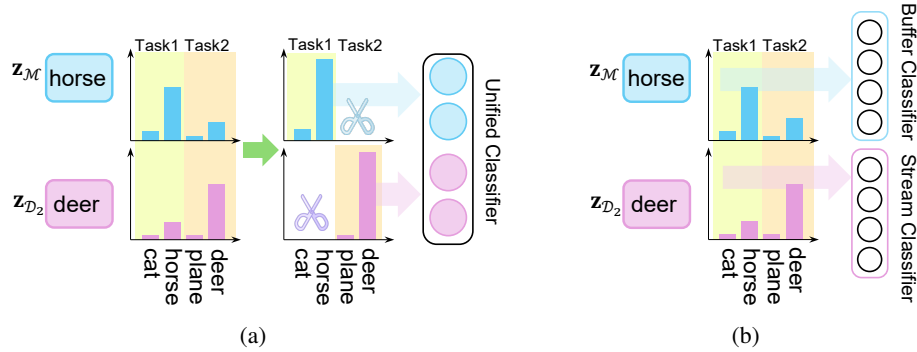


Figure 3: **Comparison between two training separation schemes.** (a) Exclusive separation [3] within a single classifier. (b) Inclusive separation with dual classifiers.

4.1 Training Separation with Dual Classifiers

The major obstacle of previous training distinction approaches is that two exclusive training schemes must compete in a single classifier. As illustrated in Figure 3(a), since both a buffer sample (e.g., a *horse* image) and a new sample (e.g., a *deer* image) share the same classifier, training separation must be exclusive in a way that each loss corresponds to either old classes or new classes, making it challenging to learn knowledge across tasks (e.g., relationship between *horse* and *deer*). Yet, without training distinction, this unified classifier can quickly get biased toward new classes.

Dual Classifiers for Training. Based on the above motivation, our method proposes dual classifiers (DC) with the same structure, replacing the single classifier. These two independent classifiers, referred to as the stream classifier and the buffer classifier, are dedicated to the conflicting tasks of knowledge acquisition and preservation, respectively. Specifically, the stream classifier, parameterized by \mathbf{W}_{str} , primarily processes incoming batches (i.e., \mathcal{B}_D) from the data stream, whereas the buffer classifier, parameterized by \mathbf{W}_{buf} , is fully responsible for learning from buffer batches (i.e., \mathcal{B}_M). For the structure of each classifier, we adopt the idea of using cosine normalization [24, 25] that can eliminate the bias caused by difference in magnitudes, thereby alleviating imbalance. Formally, each classifier is defined as:

$$f(\mathbf{z}; \mathbf{W}) = \eta \cdot \cos_vec(\mathbf{z}, \mathbf{W}), \quad (1)$$

where η is a trainable scaling factor for each classifier and $\text{cos_vec}(\mathbf{z}, \mathbf{W})$ returns a vector in which each element computed as the cosine similarity between \mathbf{z} and each class vector of \mathbf{W} . As shown in Figure 2, both classifiers still share the feature extractor, from which we obtain the feature representations $\mathbf{z}_{\mathcal{D}}$ of incoming batches and those $\mathbf{z}_{\mathcal{M}}$ of buffer batches. Then, as indicated by the green solid arrows in Figure 2, $\mathbf{z}_{\mathcal{D}}$ and $\mathbf{z}_{\mathcal{M}}$ are fed into their respective classifiers to compute the logits and cross-entropy losses.

This structural separation clearly allows the independent training of two tasks of knowledge acquisition and preservation without interference. Moreover, as illustrated in Figure 3(b), each task can still incorporate logit values from both old classes (e.g., *cat* and *horse*) and new classes (e.g., *plane* and *deer*), thereby facilitating the learning of relational knowledge (e.g., high relevance between *deer* and *horse*) across all classes. Such relationship information is particularly important for the feature extractor, which is shared by two classifiers, to learn better representation, aligning with the objective of feature enhancement.

Separation Smoothing. With dual classifiers, we define the loss function \mathcal{L}_{DC} to train all of Φ , \mathbf{W}_{buf} , and \mathbf{W}_{str} :

$$\mathcal{L}_{DC} = \mathcal{L}_{CE_{str}^{\mathcal{D}}} + \alpha \mathcal{L}_{CE_{str}^{\mathcal{M}}} + (1 - \alpha) \mathcal{L}_{CE_{buf}^{\mathcal{M}}}, \quad (2)$$

where the subscript *str* or *buf* refers to the stream or buffer classifier, and the superscript \mathcal{D} or \mathcal{M} indicates whether the loss is calculated based on the stream features $\mathbf{z}_{\mathcal{D}}$ or buffer features $\mathbf{z}_{\mathcal{M}}$. Note that this is a more refined version that can finely control the degree of separation by adjusting a control coefficient α . When $\alpha = 0$, it implies complete separation, whereas $\alpha \in (0, 1)$ makes this separation smoother in a way that some buffer features can be fed into the stream classifier as well as the buffer classifier, which is indicated by the green dotted arrow in Figure 2. However, even in this smoother version, the buffer classifier is not designed to handle stream features for securing high stability.

Notably, our \mathcal{L}_{DC} loss is entirely based on cross-entropy loss, from which the shared feature extractor can effectively be trained without extensive sample comparisons with the help of dual classifiers. Thus, we still take the benefit of cross-entropy learning as in existing training distinction methods, while enabling to obtain an improved feature extractor as in feature enhancement methods.

NCM Classifier for Inference. After training the feature extractor with dual classifiers using \mathcal{L}_{DC} , we employ the NCM classifier for making inference. This is because NCM is known to be more robust against potential biases in trained classifiers, as noted by [11], as long as the feature extractor can generate well-discriminated feature embeddings. To be shown by our experimental results in Table 2, our BOIL method takes the best out of NCM possibly due to its well-trained feature extractor.

4.2 Implicit Knowledge Interaction

Although our \mathcal{L}_{DC} loss provides a way of knowledge exchange by mixing stream samples and buffer samples when $\alpha \in (0, 1)$, relying solely on this mixing strategy cannot resolve the imbalance problem, as in the baseline ER method. Therefore, we propose implicit techniques that enable effective knowledge exchange between the buffer classifier and the stream classifier, namely (i) applying proxy-anchor loss to the training of the stream classifier along with the feature extractor, which supports forward transfer, and (ii) momentum-based updating to the buffer classifier from the stream classifier for backward transfer.

Redesigned Proxy-Anchor Loss. In our separated learning scheme with DC, the stream classifier may not effectively acquire the knowledge of buffer samples, as it is designed to guarantee such independent learning without any interference. However, the ability of forward transfer is essential in OCIL, where each stream batch contains only a small number of samples. To this end, we suggest using our redesigned version of proxy-anchor loss (PAL) [16] for the stream classifier to implicitly utilize knowledge from buffer features. The main idea is to let each class vector of the stream classifier, denoted as $\mathbf{w} \in \mathbf{W}_{str}$, be a proxy of the class during training with features of each buffer batch $\mathcal{B}_{\mathcal{M}}$ using proxy-anchor loss, replacing randomly initialized proxies in the vanilla proxy-anchor loss. We use $\mathcal{Z}_{\mathcal{M}}$ to denote the set of buffer features corresponding to $\mathcal{B}_{\mathcal{M}}$. For each $\mathcal{Z}_{\mathcal{M}}$, we define our redesigned proxy-anchor loss \mathcal{L}_{PAL} as follows:

$$\begin{aligned} \mathcal{L}_{PAL} = & \frac{1}{|\mathbf{W}_{str}^+|} \sum_{\mathbf{w} \in \mathbf{W}_{str}^+} \log(1 + \sum_{\mathbf{z} \in \mathcal{Z}_{\mathcal{M}}^+} e^{-\gamma(\langle \bar{\mathbf{z}}, \bar{\mathbf{w}} \rangle - \delta)}) \\ & + \frac{1}{|\mathbf{W}_{str}|} \sum_{\mathbf{w} \in \mathbf{W}_{str}} \log(1 + \sum_{\mathbf{z} \in \mathcal{Z}_{\mathcal{M}}^-} e^{\gamma(\langle \bar{\mathbf{z}}, \bar{\mathbf{w}} \rangle + \delta)}), \end{aligned} \quad (3)$$

where $\delta > 0$ is a margin, $\gamma > 0$ is a constant scaling factor, determining how strongly pulling or pushing embedding vectors, and $\langle \bar{\mathbf{z}}, \bar{\mathbf{w}} \rangle$ represents the cosine similarity between \mathbf{z} and \mathbf{w} . \mathbf{W}_{str}^+ denotes positive proxies corresponding

to the classes in the buffer batch. With respect to each proxy \mathbf{w} , the set of buffer features $\mathbf{Z}_{\mathcal{M}}$ is also divided into its positive and negative subsets, $\mathbf{Z}_{\mathcal{M}_w}^+$ and $\mathbf{Z}_{\mathcal{M}_w}^-$, respectively.

By minimizing \mathcal{L}_{PAL} , the stream classifier can fully utilize the knowledge of buffer samples, without explicitly training them on it using cross-entropy loss. Furthermore, previously trained but potentially removed samples from the buffer can still interact with remaining ones through proxy anchors in the stream classifier. This not only improves the knowledge consolidation in the feature space, but also makes the stream classifier more discriminative.

Momentum Updating. Lastly, in order to gradually transfer acquired knowledge from the stream classifier to the buffer classifier, we employ a momentum updating mechanism as:

$$\mathbf{W}_{buf} \leftarrow m\mathbf{W}_{buf} + (1 - m)\mathbf{W}_{str}, \quad (4)$$

where m is a momentum coefficient that controls the rate of update for the buffer classifier, typically set close to 1 (e.g., 0.99 in our experiments). This update is performed at the end of each training step, following the processing of each mini-batch, which contains a few stream and buffer samples (e.g., 10 of each in our experiments).

4.3 The Overall Process of BOIL

The overall process of BOIL is illustrated in Figure 2. BOIL comprises a shared feature extractor h , dual classifiers $f(\mathbf{z}; \mathbf{W}_{str/buf})$ and implicit knowledge interaction modules. Combining all our components, we present the final loss of our BOIL method as follows:

$$\mathcal{L}_{BOIL} = \mathcal{L}_{DC} + \beta\mathcal{L}_{PAL}, \quad (5)$$

where β is a hyperparameter. Our BOIL method trains a balanced online class-incremental learner through widely used cross-entropy loss together with redesigned proxy-anchor loss. More detailed steps are presented in the Appendix.

5 Experiments

5.1 Experimental Setup

Datasets. We use three real-world benchmark datasets in image classification. Following [7, 23], **Split CIFAR-10** is constructed by splitting CIFAR-10 [26] into 5 disjoint tasks, 2 classes per task. Both **Split CIFAR-100** and **Split Mini-ImageNet** contain 10 disjoint tasks, 10 classes per task, by splitting CIFAR-100 [26] and Mini-ImageNet [27], respectively.

Baselines. We compare our BOIL method with the following replay-based methods in the OCIL setting: ER [2], GSS [8], MIR [6], A-GEM [28], Gdumb [29], ASER [7], SS-IL [3], ER-DVC [23], ER-ACE [4], OCM [13], PCR [12] and LODE [9]. We also include FINE-TUNE as a non-replay baseline for comparison.

Evaluation Metrics. For performance assessment, we use three metrics commonly used in OCIL [7, 30, 31]: *average accuracy* (AA), *average forgetting* (AF), and *average intransigence* (AI). Intuitively, the higher AA indicates better overall performance, yet the lower AF and AI imply better stability and better plasticity, respectively. To provide their formal definitions, we first let $a_{k,j} \in [0, 1]$ to denote the task-wise classification accuracy for the j -th task after learning $k \geq j$ continual tasks. According to the single-head evaluation setup [30], each prediction is made across all classes without being aware of task identification. Then, at the k -th task, three metrics are defined as follows [31]: $AA_k = \frac{1}{k} \sum_{j=1}^k a_{k,j}$, $AF_k = \frac{1}{k-1} \sum_{j=1}^{k-1} f_{j,k}$, and $AI_k = \frac{1}{k} \sum_{j=1}^k a_j^* - a_{j,j}$, where (i) $f_{j,k} = \max_{i \in \{1, \dots, k-1\}} (a_{i,j} - a_{k,j})$ for $\forall j < k$, and (ii) a_j^* indicates an empirical upper-bound for the task-wise accuracy of the j -th task, which is obtained from a purely fine-tuned model with respect to \mathcal{D}_j without using any other loss terms. In terms of their value ranges, we have $AA \in [0, 1]$, $AF \in [-1, 1]$, and $AI \in [-1, 1]$.

Implementation Details. Following the common architecture in OCIL [11, 23, 12], we utilize Reduced ResNet-18 [32] as the feature extractor. For batch size, each stream batch contains 10 images drawn from the data stream, while 10 samples are randomly retrieved from the buffer to form a buffer batch. In our BOIL method, we set $m = 0.99$ in Eq. (4), $\gamma = 32$ and $\delta = 0.1$ in Eq. (5) for all datasets. For Split CIFAR-100 and Split Mini-ImageNet, α in Eq. (2) and β in Eq. (5) are set to 0.5 and 0.2, respectively, whereas they are set to 0 and 0.1 for Split CIFAR-10. We reproduce all the evaluations in a consistent environment, where NVIDIA Geforce 3090 GPU and PyTorch toolbox are utilized. Each measurement in all experimental results is the average along with its corresponding standard deviation over 10 independent runs, where each run shuffles classes when splitting datasets. Full implementation details are presented in the Appendix.

Table 1: **Average accuracy at the end of training on three datasets.** The best scores are highlighted in **boldface**, while the runner-up scores are underlined. ‘T’ and ‘F’ indicate two categories: *training distinction* and *feature enhancement*, respectively.

| Method | Split CIFAR-100 | | | Split CIFAR-10 | | | Split Mini-ImageNet | | |
|--------------------|-----------------------|-----------------------|-----------------------|-----------------------|-----------------------|-----------------------|-----------------------|-----------------------|-----------------------|
| | $\mathcal{M} = 1k$ | $\mathcal{M} = 2k$ | $\mathcal{M} = 5k$ | $\mathcal{M} = 0.2k$ | $\mathcal{M} = 0.5k$ | $\mathcal{M} = 1k$ | $\mathcal{M} = 1k$ | $\mathcal{M} = 2k$ | $\mathcal{M} = 5k$ |
| FINE-TUNE | | 5.2 \pm 0.6 | | | 17.4 \pm 0.8 | | | 4.6 \pm 0.7 | |
| ER | 16.5 \pm 0.6 | 19.7 \pm 1.0 | 20.4 \pm 1.9 | 38.1 \pm 4.5 | 42.8 \pm 5.4 | 46.9 \pm 5.2 | 14.2 \pm 1.3 | 16.1 \pm 1.2 | 14.3 \pm 2.4 |
| GSS (T) | 16.6 \pm 0.9 | 18.7 \pm 1.3 | 18.2 \pm 0.9 | 25.2 \pm 2.0 | 30.2 \pm 2.4 | 38.7 \pm 4.0 | 13.0 \pm 0.9 | 14.7 \pm 1.9 | 14.6 \pm 2.1 |
| MIR (T) | 17.9 \pm 0.9 | 20.3 \pm 1.4 | 20.2 \pm 1.8 | 37.2 \pm 3.3 | 43.7 \pm 4.4 | 46.3 \pm 3.6 | 15.2 \pm 0.7 | 16.1 \pm 1.5 | 16.8 \pm 2.1 |
| A-GEM (T) | 5.3 \pm 0.4 | 5.0 \pm 0.5 | 5.7 \pm 0.3 | 17.4 \pm 1.0 | 17.1 \pm 1.3 | 17.6 \pm 1.0 | 4.5 \pm 0.5 | 4.9 \pm 0.5 | 4.9 \pm 0.4 |
| Gdumb (T) | 10.8 \pm 0.6 | 16.7 \pm 0.5 | 29.2 \pm 0.8 | 28.7 \pm 1.8 | 37.4 \pm 1.8 | 45.0 \pm 1.3 | 9.2 \pm 0.5 | 15.7 \pm 0.4 | 27.2 \pm 1.6 |
| SCR (F) | 13.6 \pm 0.9 | 14.9 \pm 0.8 | 15.8 \pm 0.6 | 46.1 \pm 2.1 | 54.8 \pm 1.5 | 57.8 \pm 1.6 | 13.0 \pm 0.6 | 14.6 \pm 0.4 | 15.9 \pm 0.6 |
| ASER (T) | 19.2 \pm 0.7 | 21.9 \pm 0.9 | 25.5 \pm 1.4 | 30.4 \pm 2.4 | 36.0 \pm 3.4 | 44.5 \pm 2.8 | 14.6 \pm 1.2 | 16.5 \pm 0.8 | 20.1 \pm 1.1 |
| SS-IL (T) | 21.1 \pm 0.8 | 22.5 \pm 0.7 | 22.3 \pm 0.6 | 41.3 \pm 1.1 | 43.8 \pm 2.0 | 47.7 \pm 2.0 | 19.0 \pm 1.1 | 20.5 \pm 1.0 | 20.3 \pm 0.8 |
| ER-DVC (T) | 19.3 \pm 1.2 | 22.2 \pm 1.5 | 23.9 \pm 1.4 | 45.6 \pm 2.8 | 45.4 \pm 3.5 | 52.1 \pm 2.8 | 17.0 \pm 1.0 | 17.6 \pm 1.6 | 18.8 \pm 1.7 |
| ER-ACE (T) | 23.0 \pm 0.4 | 25.6 \pm 0.8 | 27.7 \pm 0.9 | 48.0 \pm 2.2 | 54.0 \pm 1.0 | 58.6 \pm 1.7 | 20.5 \pm 1.7 | 23.6 \pm 1.4 | 25.2 \pm 1.9 |
| OCM (T, F) | 15.5 \pm 0.8 | 17.6 \pm 0.7 | 18.2 \pm 0.6 | 40.7 \pm 2.3 | 46.9 \pm 3.5 | 51.6 \pm 3.2 | 13.4 \pm 0.6 | 15.1 \pm 1.0 | 16.6 \pm 0.7 |
| PCR (F) | 24.6 \pm 0.7 | 27.3 \pm 0.9 | 29.6 \pm 0.9 | 50.6 \pm 1.6 | 54.3 \pm 0.9 | 58.2 \pm 2.6 | 23.9 \pm 0.6 | 26.7 \pm 0.7 | 27.3 \pm 0.8 |
| LODE (T) | 24.4 \pm 1.1 | 26.5 \pm 1.1 | 29.0 \pm 1.1 | 51.1 \pm 2.1 | 56.9 \pm 2.9 | 59.2 \pm 1.7 | 22.1 \pm 0.7 | 25.3 \pm 1.0 | 27.8 \pm 0.9 |
| BOIL (ours) | 26.3 \pm 0.8 | 30.3 \pm 0.7 | 33.1 \pm 1.0 | 51.5 \pm 1.0 | 57.5 \pm 0.6 | 61.4 \pm 1.3 | 23.9 \pm 0.6 | 27.0 \pm 0.6 | 28.5 \pm 0.5 |

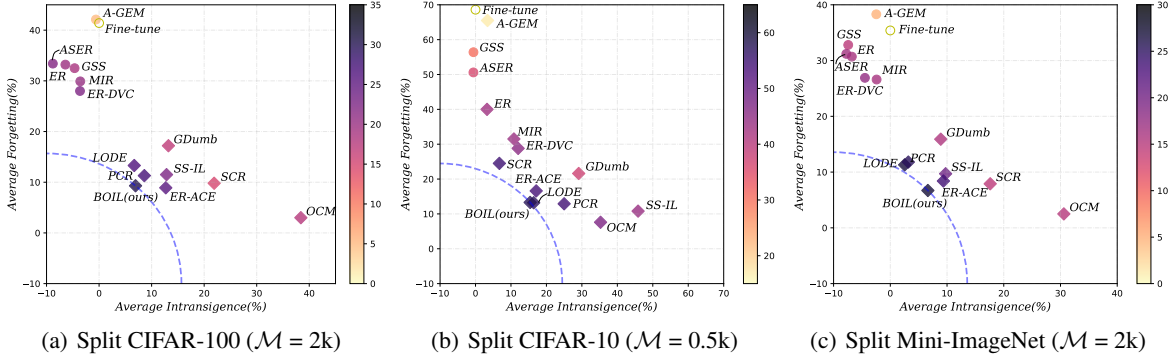


Figure 4: **Balance between stability and plasticity.** Each graph plots average intransigence (AI) on the x-axis, which measures plasticity, and average forgetting (AF) on the y-axis, which measures stability. Both AI and AF are equally scaled in $[-1, 1]$, with lower values indicating better plasticity and stability, respectively. Different colors represent levels of average accuracy.

5.2 Performance Comparison

Overall Performance. Table 1 summarizes overall performance evaluation using three datasets, where we present the average accuracy of each model at the end of training over all tasks with different buffer sizes. Our BOIL consistently achieves the best performance among all compared methods in all settings, mostly followed by PCR [12]. Training distinction methods generally tend to show unsatisfactory performance with clear margins except for LODE [9], compared to BOIL. Either SS-IL [3] or ER-ACE [4] relies on exclusive loss separation, leading to less competitive performance, while LODE manages to further improve the performance by relaxed loss separation. In the category of feature enhancement, PCR takes the best position by leveraging proxies in metric learning, but SCR [11] seems to suffer from too few samples in a mini-batch to train with its supervised contrastive loss. Every method obviously shows better performance as buffer size increases, but our BOIL method takes the best use of knowledge from buffer samples, further enlarging the performance gap with a larger buffer space.

Balance of Stability and Plasticity. To evaluate the balance between plasticity and stability, Figure 4 displays *interplay graphs* [30], which plot each method based on two key metrics: average forgetting (AF) and average intransigence (AI). We also use different colors to show different levels of average accuracy (AA). Both AF and AI have the same range $[-1, 1]$, where lower values represent better stability and plasticity, respectively. Note that although AF and AI can technically be negative, a zero value already indicates no deviation from the ideal performance achievable through joint training with the entire dataset. In all the graphs, our BOIL method is clearly positioned closest to the bottom-left corner, and is represented with the darkest color. This demonstrates that BOIL not only outperforms existing methods in terms

Table 2: **Average accuracy with or without using the NCM classifier on Split Mini-ImageNet with various buffer sizes.**

| Method | $\mathcal{M} = 1k$ | $\mathcal{M} = 2k$ | $\mathcal{M} = 5k$ |
|--------------------|----------------------------------|----------------------------------|----------------------------------|
| ER | 14.2 ± 1.3 | 16.1 ± 1.2 | 14.3 ± 2.4 |
| ER + NCM | 18.9 ± 1.1 | 21.4 ± 1.4 | 20.9 ± 2.2 |
| SCR | 13.0 ± 0.6 | 14.6 ± 0.4 | 15.9 ± 0.6 |
| ER-ACE | 20.5 ± 1.7 | 23.6 ± 1.4 | 25.2 ± 1.9 |
| ER-ACE + NCM | 21.9 ± 0.7 | 25.1 ± 0.6 | 26.7 ± 0.7 |
| PCR | 23.9 ± 0.6 | 26.7 ± 0.7 | 27.3 ± 0.8 |
| PCR + NCM | 23.4 ± 0.5 | 26.0 ± 0.5 | 27.4 ± 0.4 |
| LODE | 22.1 ± 0.7 | 25.3 ± 1.0 | 27.8 ± 0.9 |
| LODE + NCM | 22.9 ± 0.3 | 26.3 ± 0.5 | 28.4 ± 0.7 |
| BOIL (ours) | 23.9 ± 0.6 | 27.0 ± 0.6 | 28.5 ± 0.5 |

Table 3: **Ablation study on Split Mini-ImageNet ($\mathcal{M}=1k$).** “w/o all” represents vanilla ER with the NCM classifier.

| Method | AA \uparrow | AF \downarrow | AI \downarrow |
|--------------------|----------------------------------|---------------------------------|---------------------------------|
| BOIL (ours) | 23.9 ± 0.6 | 9.9 ± 0.7 | 6.3 ± 8.6 |
| w/o DC & MU | 18.1 ± 1.3 | 7.4 ± 0.4 | 14.8 ± 8.4 |
| w/o MU | 23.2 ± 0.6 | 9.9 ± 0.8 | 6.9 ± 8.9 |
| w/o PAL | 22.8 ± 0.5 | 10.4 ± 0.7 | 7.0 ± 8.4 |
| w/o all | 18.9 ± 1.1 | 8.1 ± 0.9 | 13.1 ± 8.4 |

of overall performance, but also consistently achieves the best balance between stability and plasticity. Methods like OCM [13] tend to prioritize stability at the expense of plasticity. In contrast, methods with negative AI values (depicted as circular points), such as vanilla ER [2], excessively focus on plasticity, yet they suffer from severe forgetting with respect to AF, consequently failing to secure high AAs. Overall, maintaining balance is crucial for achieving high performance in OCIL, as more balanced methods tend to have darker-colored points, corresponding to higher AAs, with BOIL leading the way, followed by LODE, PCR and ER-ACE.

5.3 Ablation Studies

Impact of Each Component. Table 3 presents the results of our ablation study on Split Mini-ImageNet with 1k buffer samples. To assess the impact of different components in the BOIL method, we examine performance changes after the removal of individual components: Dual Classifiers (DC), redesigned Proxy-Anchor Loss (PAL), and Momentum Updating (MU), while commonly using the NCM classifier for inference. We first verify the impact of DC by removing DC and MU together, as MU is a backward transfer strategy that depends on DC and cannot function independently. The results, indicated by the reduced AA and increased AI in the ‘w/o DC & MU’ setting, demonstrate the critical role of DC in enhancing plasticity as well as accuracy. This is partly because removing DC also includes discarding its underlying structure using cosine normalization. The comparison between BOIL and ‘w/o MU’ shows that MU further improves both plasticity and accuracy when combined with DC. Removing PAL also results in a decline in both stability and plasticity corresponding to increased AF and AI values in ‘w/o PAL’, leading to a decrease in AA. The ‘w/o all’ setting, which represents vanilla ER with NCM, exhibits the worst overall performance. This indicates that every component is essentially required to obtain the final performance and to maintain a good balance between AF and AI.

Impact of NCM. From the result of the ‘w/o all’ setting in Table 3, the NCM classifier itself seems to be effective at enhancing stability even when used with vanilla ER. Motivated by this, in Table 2, we further examine whether NCM can similarly enhance performance when combined with competitive state-of-the-art methods on Split Mini-ImageNet with varying buffer sizes. Note that the NCM classifier is already embedded in the SCR method as well as in our BOIL method. As presented in Table 2, our BOIL method still outperforms all the compared methods regardless of whether they use NCM or not. While NCM generally improves classification accuracy, its impact varies depending on the underlying training methods. Specifically, vanilla ER takes the greatest benefit of using NCM, probably because the NCM classifier can mitigate class bias toward new tasks, which is a significant issue in the linear classifier of vanilla ER. In contrast, the performance improvement is less pronounced or occasionally negative in more advanced methods like ER-ACE and PCR. Notably, compared to SCR, which also utilizes NCM in its methodology, BOIL substantially improves the performance with the help of our proposed techniques.

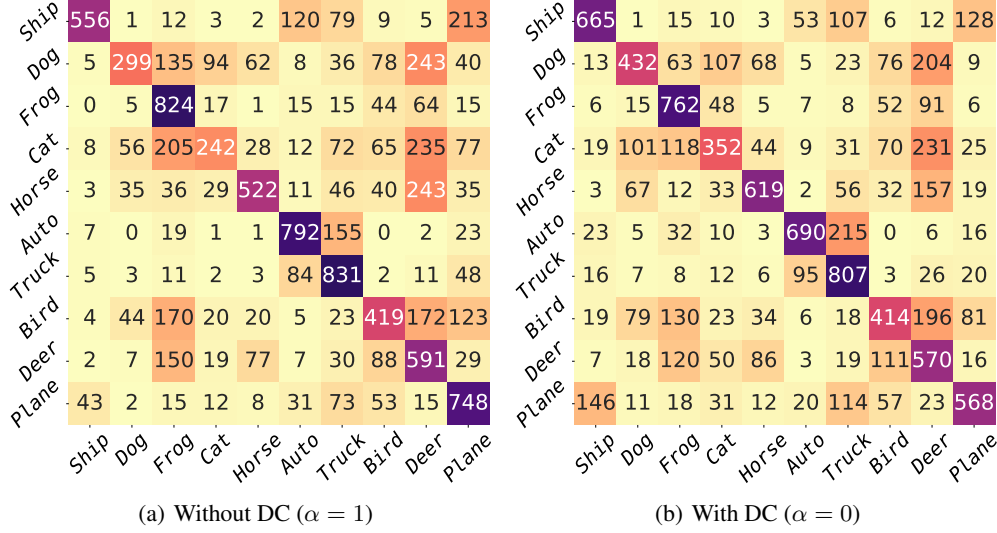


Figure 5: **Confusion matrix with or without using dual classifiers in Split CIFAR-10 ($\mathcal{M} = 1k$, $\beta = 0$, and $m = 1$).** The X-axis is the predicted label and the Y-axis is the ground truth.

Table 4: **Balanced performance with or without using dual classifiers in Split CIFAR-10 ($\mathcal{M} = 1k$, $\beta = 0$, and $m = 1$).**

| Method | AA \uparrow | STD \downarrow | Max | Min |
|--------|---------------|------------------|------|------|
| w/o DC | 58.2 | 21.6 | 83.1 | 24.2 |
| w/ DC | 58.8 | 15.1 | 80.7 | 35.2 |

5.4 Effectiveness of Inclusive Training Separation

Although we have confirmed the effectiveness of dual classifiers (DC) in our ablation study shown in Table 3, we further conduct an in-depth analysis on the benefit of our *inclusive training separation* using DC. To this end, in Figure 5, we present the confusion matrix, when solely applying DC to the baseline method (i.e., vanilla ER with the NCM classifier) on Split CIFAR-10 with a buffer size of 1k, in comparison with those without using DC. In confusion matrices, the x-axis represents predictions made by the models and the y-axis denotes true class labels, where we can also get class-wise accuracies from the diagonal values. The results are obtained by making predictions against 10k test samples, 1k per class, after training five incremental tasks of Split CIFAR-10, which are (*ship*, *dog*), (*frog*, *cat*), (*horse*, *automobile*), (*truck*, *bird*), and (*deer*, *airplane*) in order.

Reducing Bias Towards New Tasks. Our first observation from Figure 5 is that predictions for the newest classes, *deer* and *airplane*, are reduced when using DC, as shown in Figure 5(b) (2,404 predictions in total), compared to when DC is not used, as shown in Figure 5(a) (2,932 predictions in total). This reduction indicates that our training separation effectively mitigates bias towards new tasks. Furthermore, this approach enhances the precision of predictions for these new classes: the precision for *airplane* improves from $\frac{748}{1,351} = 55.4\%$ to $\frac{568}{888} = 64.0\%$, and for *deer* from $\frac{591}{1,581} = 37.4\%$ to $\frac{570}{1,516} = 37.6\%$.

Capturing Semantic Relationship. Figure 5 also indicates that our inclusive separation effectively captures semantic relationships between classes, as expected in Figure 3. For example, predictions for semantically similar classes, such as *automobile* and *truck* or *cat* and *dog*, become more correlated in Figure 5(b) compared to Figure 5(a). This high level of correlation suggests that our inclusive separation scheme makes it more difficult for the model to differentiate between similar classes. However, this increased correlation is what we intend to achieve for better feature embeddings, as it helps reduce incorrect predictions for unrelated classes, thereby enhancing overall accuracy. This improvement is evident in Figure 5, where there is a notable reduction in incorrect predictions to unrelated classes, such as from *cat* to *frog* (from 205 in Figure 5(a) to 118 in Figure 5(b)), despite the increased misclassification between similar classes like *cat* and *dog*. Consequently, as observed from the diagonal values, the class-wise accuracy for *cat* increases from 24.2% to 35.2%, and for *dog*, it rises from 29.9% to 43.2%. Moreover, we present the average accuracy (AA) among 10 classes, the corresponding standard deviation (STD), the maximum and minimum class-wise accuracy in

Table 4. The method fully employing DC not only maintains a better overall accuracy, but also exhibits more balanced performance across all classes, from the smaller STD, the smaller Max, and the larger Min values, compared to the version without DC. This shows the effectiveness of inclusive separation of DC in improving overall performance as well as achieving balanced outcomes.

6 Conclusion

In this work, we proposed a novel method for online class-incremental learning, named BOIL, to overcome the limitations of existing replay-based methods, which often favor either plasticity or stability. BOIL suggests employing dual classifiers for inclusive separation of learning new samples from replaying buffer samples, thereby mitigating bias toward new tasks yet effectively consolidating knowledge across different tasks. By introducing implicit knowledge exchange between the dual classifiers, BOIL facilitates both forward and backward transfer throughout the incremental learning process. Empirical results demonstrate that BOIL achieves the best classification performance by providing the most balanced learner for OCIL.

References

- [1] Mermillod, Martial, Bugaiska, Aurélia, and Patrick Bonin. The stability-plasticity dilemma: Investigating the continuum from catastrophic forgetting to age-limited learning effects, 2013.
- [2] Arslan Chaudhry, Marcus Rohrbach, Mohamed Elhoseiny, Thalaiyasingam Ajanthan, Puneet K Dokania, Philip HS Torr, and Marc’Aurelio Ranzato. On tiny episodic memories in continual learning. *arXiv preprint arXiv:1902.10486*, 2019.
- [3] Hongjoon Ahn, Jihwan Kwak, Subin Lim, Hyeonsu Bang, Hyojun Kim, and Taesup Moon. SS-IL: separated softmax for incremental learning. In *2021 IEEE/CVF International Conference on Computer Vision, ICCV 2021, Montreal, QC, Canada, October 10-17, 2021*, pages 824–833. IEEE, 2021.
- [4] Lucas Caccia, Rahaf Aljundi, Nader Asadi, Tinne Tuytelaars, Joelle Pineau, and Eugene Belilovsky. New insights on reducing abrupt representation change in online continual learning. In *The Tenth International Conference on Learning Representations, ICLR 2022, Virtual Event, April 25-29, 2022*. OpenReview.net, 2022.
- [5] Guoqiang Liang, Zhaojie Chen, Zhaoqiang Chen, Shiyu Ji, and Yanning Zhang. New insights on relieving task-recency bias for online class incremental learning. *IEEE Trans. Circuits Syst. Video Technol.*, 34(5):3451–3464, 2024.
- [6] Rahaf Aljundi, Eugene Belilovsky, Tinne Tuytelaars, Laurent Charlin, Massimo Caccia, Min Lin, and Lucas Page-Caccia. Online continual learning with maximal interfered retrieval. In Hanna M. Wallach, Hugo Larochelle, Alina Beygelzimer, Florence d’Alché-Buc, Emily B. Fox, and Roman Garnett, editors, *Advances in Neural Information Processing Systems 32: Annual Conference on Neural Information Processing Systems 2019, NeurIPS 2019, December 8-14, 2019, Vancouver, BC, Canada*, pages 11849–11860, 2019.
- [7] Dongsu Shim, Zheda Mai, Jihwan Jeong, Scott Sanner, Hyunwoo Kim, and Jongseong Jang. Online class-incremental continual learning with adversarial shapley value. In *Thirty-Fifth AAAI Conference on Artificial Intelligence, AAAI 2021, Thirty-Third Conference on Innovative Applications of Artificial Intelligence, IAAI 2021, The Eleventh Symposium on Educational Advances in Artificial Intelligence, EAAI 2021, Virtual Event, February 2-9, 2021*, pages 9630–9638. AAAI Press, 2021.
- [8] Rahaf Aljundi, Min Lin, Baptiste Goujaud, and Yoshua Bengio. Gradient based sample selection for online continual learning. In Hanna M. Wallach, Hugo Larochelle, Alina Beygelzimer, Florence d’Alché-Buc, Emily B. Fox, and Roman Garnett, editors, *Advances in Neural Information Processing Systems 32: Annual Conference on Neural Information Processing Systems 2019, NeurIPS 2019, December 8-14, 2019, Vancouver, BC, Canada*, pages 11816–11825, 2019.
- [9] Yan-Shuo Liang and Wu-Jun Li. Loss decoupling for task-agnostic continual learning. In *Advances in Neural Information Processing Systems 36: Annual Conference on Neural Information Processing Systems 2023, NeurIPS 2023, New Orleans, LA, USA, December 10 - 16, 2023*, 2023.
- [10] Sylvestre-Alvise Rebuffi, Alexander Kolesnikov, Georg Sperl, and Christoph H. Lampert. icarl: Incremental classifier and representation learning. In *2017 IEEE Conference on Computer Vision and Pattern Recognition, CVPR 2017, Honolulu, HI, USA, July 21-26, 2017*, pages 5533–5542. IEEE Computer Society, 2017.
- [11] Zheda Mai, Ruiwen Li, Hyunwoo Kim, and Scott Sanner. Supervised contrastive replay: Revisiting the nearest class mean classifier in online class-incremental continual learning. In *IEEE Conference on Computer Vision and*

- Pattern Recognition Workshops, CVPR Workshops 2021, virtual, June 19-25, 2021*, pages 3589–3599. Computer Vision Foundation / IEEE, 2021.
- [12] Huiwei Lin, Baoquan Zhang, Shanshan Feng, Xutao Li, and Yunming Ye. PCR: proxy-based contrastive replay for online class-incremental continual learning. In *IEEE/CVF Conference on Computer Vision and Pattern Recognition, CVPR 2023, Vancouver, BC, Canada, June 17-24, 2023*, pages 24246–24255. IEEE, 2023.
 - [13] Yiduo Guo, Bing Liu, and Dongyan Zhao. Online continual learning through mutual information maximization. In Kamalika Chaudhuri, Stefanie Jegelka, Le Song, Csaba Szepesvári, Gang Niu, and Sivan Sabato, editors, *International Conference on Machine Learning, ICML 2022, 17-23 July 2022, Baltimore, Maryland, USA*, volume 162 of *Proceedings of Machine Learning Research*, pages 8109–8126. PMLR, 2022.
 - [14] Yujie Wei, Jiaxin Ye, Zhizhong Huang, Junping Zhang, and Hongming Shan. Online prototype learning for online continual learning. In *IEEE/CVF International Conference on Computer Vision, ICCV 2023, Paris, France, October 1-6, 2023*, pages 18718–18728. IEEE, 2023.
 - [15] Thomas Mensink, Jakob Verbeek, Florent Perronnin, and Gabriela Csurka. Distance-based image classification: Generalizing to new classes at near-zero cost. *IEEE Trans. Pattern Anal. Mach. Intell.*, 35(11):2624–2637, 2013.
 - [16] Sungyeon Kim, Dongwon Kim, Minsu Cho, and Suha Kwak. Proxy anchor loss for deep metric learning. In *2020 IEEE/CVF Conference on Computer Vision and Pattern Recognition, CVPR 2020, Seattle, WA, USA, June 13-19, 2020*, pages 3235–3244. Computer Vision Foundation / IEEE, 2020.
 - [17] Bowen Zhao, Xi Xiao, Guojun Gan, Bin Zhang, and Shu-Tao Xia. Maintaining discrimination and fairness in class incremental learning. In *2020 IEEE/CVF Conference on Computer Vision and Pattern Recognition, CVPR 2020, Seattle, WA, USA, June 13-19, 2020*, pages 13205–13214. Computer Vision Foundation / IEEE, 2020.
 - [18] Pietro Buzzega, Matteo Boschini, Angelo Porrello, Davide Abati, and Simone Calderara. Dark experience for general continual learning: a strong, simple baseline. In Hugo Larochelle, Marc’Aurelio Ranzato, Raia Hadsell, Maria-Florina Balcan, and Hsuan-Tien Lin, editors, *Advances in Neural Information Processing Systems 33: Annual Conference on Neural Information Processing Systems 2020, NeurIPS 2020, December 6-12, 2020, virtual*, 2020.
 - [19] Shipeng Yan, Jiangwei Xie, and Xuming He. DER: dynamically expandable representation for class incremental learning. In *IEEE Conference on Computer Vision and Pattern Recognition, CVPR 2021, virtual, June 19-25, 2021*, pages 3014–3023. Computer Vision Foundation / IEEE, 2021.
 - [20] Gido M. van de Ven, Tinne Tuytelaars, and Andreas S. Tolias. Three types of incremental learning. *Nat. Mac. Intell.*, 4(12):1185–1197, 2022.
 - [21] David Lopez-Paz and Marc’Aurelio Ranzato. Gradient episodic memory for continual learning. In Isabelle Guyon, Ulrike von Luxburg, Samy Bengio, Hanna M. Wallach, Rob Fergus, S. V. N. Vishwanathan, and Roman Garnett, editors, *Advances in Neural Information Processing Systems 30: Annual Conference on Neural Information Processing Systems 2017, December 4-9, 2017, Long Beach, CA, USA*, pages 6467–6476, 2017.
 - [22] Matthew Riemer, Ignacio Cases, Robert Ajemian, Miao Liu, Irina Rish, Yuhai Tu, and Gerald Tesauro. Learning to learn without forgetting by maximizing transfer and minimizing interference. In *7th International Conference on Learning Representations, ICLR 2019, New Orleans, LA, USA, May 6-9, 2019*. OpenReview.net, 2019.
 - [23] Yanan Gu, Xu Yang, Kun Wei, and Cheng Deng. Not just selection, but exploration: Online class-incremental continual learning via dual view consistency. In *IEEE/CVF Conference on Computer Vision and Pattern Recognition, CVPR 2022, New Orleans, LA, USA, June 18-24, 2022*, pages 7432–7441. IEEE, 2022.
 - [24] Chunjie Luo, Jianfeng Zhan, Xiaohe Xue, Lei Wang, Rui Ren, and Qiang Yang. Cosine normalization: Using cosine similarity instead of dot product in neural networks. In Vera Kurková, Yannis Manolopoulos, Barbara Hammer, Lazaros S. Iliadis, and Ilias Maglogiannis, editors, *Artificial Neural Networks and Machine Learning - ICANN 2018 - 27th International Conference on Artificial Neural Networks, Rhodes, Greece, October 4-7, 2018, Proceedings, Part I*, volume 11139 of *Lecture Notes in Computer Science*, pages 382–391. Springer, 2018.
 - [25] Saihui Hou, Xinyu Pan, Chen Change Loy, Zilei Wang, and Dahua Lin. Learning a unified classifier incrementally via rebalancing. In *IEEE Conference on Computer Vision and Pattern Recognition, CVPR 2019, Long Beach, CA, USA, June 16-20, 2019*, pages 831–839. Computer Vision Foundation / IEEE, 2019.
 - [26] Alex Krizhevsky, Geoffrey Hinton, et al. Learning multiple layers of features from tiny images. 2009.
 - [27] Oriol Vinyals, Charles Blundell, Tim Lillicrap, Koray Kavukcuoglu, and Daan Wierstra. Matching networks for one shot learning. In Daniel D. Lee, Masashi Sugiyama, Ulrike von Luxburg, Isabelle Guyon, and Roman Garnett, editors, *Advances in Neural Information Processing Systems 29: Annual Conference on Neural Information Processing Systems 2016, December 5-10, 2016, Barcelona, Spain*, pages 3630–3638, 2016.

- [28] Arslan Chaudhry, Marc’Aurelio Ranzato, Marcus Rohrbach, and Mohamed Elhoseiny. Efficient lifelong learning with a-gem. *arXiv preprint arXiv:1812.00420*, 2018.
- [29] Ameya Prabhu, Philip H. S. Torr, and Puneet K. Dokania. Gdumb: A simple approach that questions our progress in continual learning. In Andrea Vedaldi, Horst Bischof, Thomas Brox, and Jan-Michael Frahm, editors, *Computer Vision - ECCV 2020 - 16th European Conference, Glasgow, UK, August 23-28, 2020, Proceedings, Part II*, volume 12347 of *Lecture Notes in Computer Science*, pages 524–540. Springer, 2020.
- [30] Arslan Chaudhry, Puneet Kumar Dokania, Thalaiyasingam Ajanthan, and Philip H. S. Torr. Riemannian walk for incremental learning: Understanding forgetting and intransigence. In Vittorio Ferrari, Martial Hebert, Cristian Sminchisescu, and Yair Weiss, editors, *Computer Vision - ECCV 2018 - 15th European Conference, Munich, Germany, September 8-14, 2018, Proceedings, Part XI*, volume 11215 of *Lecture Notes in Computer Science*, pages 556–572. Springer, 2018.
- [31] Sungmin Cha, Hsiang Hsu, Taebaek Hwang, Flávio P. Calmon, and Taesup Moon. CPR: classifier-projection regularization for continual learning. In *9th International Conference on Learning Representations, ICLR 2021, Virtual Event, Austria, May 3-7, 2021*. OpenReview.net, 2021.
- [32] Kaiming He, Xiangyu Zhang, Shaoqing Ren, and Jian Sun. Deep residual learning for image recognition. In *2016 IEEE Conference on Computer Vision and Pattern Recognition, CVPR 2016, Las Vegas, NV, USA, June 27-30, 2016*, pages 770–778. IEEE Computer Society, 2016.